Proceeding *20th SEAGC - 3rd AGSSEA Conference in conjunction with 22nd Annual Indonesian National Conference on Geotechnical Engineering.* Jakarta - INDONESIA, 6 -7 November 2018. ISBN No. 978-602-17221-6-9

Volume Measurement for Heavy Pounding Induced Craters and Ground Heave

J. L. Hung[1], U. H. Amalia[1], H. C. Shih[2], and J. C. Chih[3]
[1]*Department of Civil and Construction Engineering, National Taiwan University of Science and Technology, Taipei, Taiwan*
[2]*Taiwan Building Technology Center, National Taiwan University of Science and Technology, Taipei, Taiwan*
[3]*Li-Jia Engineering Company, Taipei, Taiwan*
E-mail: amaliaula@gmail.com

ABSTRACT: Traditionally, the volume of dynamic compaction induced crater and ground heave is measured by means of level surveying and ruler measurement. However, since ground heave around the crater and the shape of the crater itself are irregular, it is not only difficult but also time-consuming to accurately measure the volume of crater and ground heave. This study proposes a method that adopts the up-to-date image processing (photogrammetry) technology to more accurately measure the crater volume and the ground heave around it. A commercial software, which is initially used for the drone, is used here to generate point cloud of the crater and its surrounding area using the images captured with a video camera or smartphone. The accuracy of this method was calibrated with a known volume box in the laboratory first before it was used in a field trial test. This paper will present and discuss the operation procedure and image processing of this method. The crater volume measured from the photogrammetry method is compared with that measured from the traditional measuring method. It is found that the volume of DC crater can be better approximated by cone shape crater than by truncated cone shape crater, which is commonly used in the DC industry and can be seriously over-estimate the actual volume of DC craters.
Keywords: crater volume, ground heave, dynamic compaction, photogrammetry method.

1. INTRODUCTION

Ground improvement by heavy poundings like dynamic compaction (DC) and rapid impact compaction (RIC) is a commonly used method for the densification of in-situ sandy soil to a large depth. After pounding, a crater on the ground is formed, and surface heaved. To evaluate the effectiveness of pounding, the volume change of crater and ground heave before and after pounding needs to be measured. Traditionally, the volume of crater and ground heave was measured using level surveying. However, since ground heaves around the crater and craters itself are irregular in shape, it is difficult to be accurately measured with traditional surveying method. This study will use the up-to-date image processing technology (photogrammetry) to measure the crater volume and the ground heave around it with reasonable accuracy. A commercial software (Pix4Dmapper) which is initially used for the drone is adopted here to generate point cloud of the crater using the images captured with a smartphone camera. In this study, the accuracy of this method was calibrated with a known volume box in the laboratory first before it was used on a pilot test project of DC and RIC densification on a land reclamation site, which was reclaimed by hydraulic fill method.

2. TEST SITE CONDITIONS

The backfill material of the reclaimed site was mostly silty sand soil pumped in by dredging boat from the nearby seabed. As shown in Table 1, from ground surface to GL-8 m, it was silty sand layer with trace of gravel and shells and N = 2~20; from GL – 8 m to GL -16 m, it was silty sand layer with trace of clay and N= 4~16; from GL -16 m to GL -25 m, it was sandy silt layer with clay and fine sand and N = 7~28; from GL -25 m ~ GL -49.4 m, it was silty sand layer with N = 14 ~ 23. The hydraulically filled sandy soil (GL to GL -16 m) was loose and sensitive to vibration; it will be very likely to liquefy during earthquake shaking. To improve the engineering properties of the reclaimed land against earthquake-induced liquefaction, the dynamic compaction (DC) and rapid impact compaction (RIC) methods (Figure 1) were tested during the pilot test of this ground improvement project.

Table 1. Simplified soil profile of the reclaimed land

Depth (m)	Soil	Thick (m)	SPT-N (Avg.)	ω (%)	γ (t/m^3)	ϕ
0 - 8	SM-1	8.0	2 – 20 (8)	4.8 ~ 33.6	1.52 ~ 2.13	30°
8 - 16	SM-2	8.0	4 – 16 (9)	12.4 ~ 32.8	1.61 ~ 2.11	30°
16 - 25	SM-3	9.0	7 – 28 (16)	11.7 ~ 39.7	1.63 ~ 2.11	32°
25 - 49.4	SM-4	24.4	14 – 23 (22)	18.3 ~ 31.4	1.69 ~ 2.11	34°

(a) Dynamic compaction (DC) (b) Rapid Impact Compaction (RIC)

Figure 1. Dynamic compaction and rapid impact compaction methods

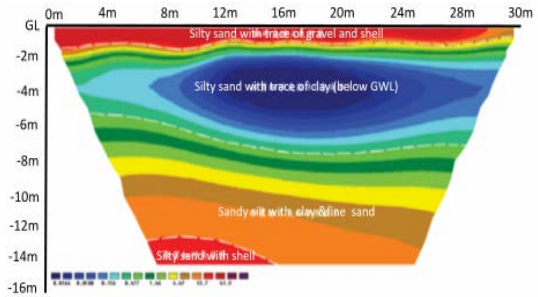

Figure 2. Electrical resistivity image profile (RIP) of reclaimed land at the test site

The SPT-N values of the hydraulically filled sandy soil at GL -5 m ~ GL -9 m (= 4 ~ 10) was weaker than the soil near the surface (GL ~ GL -5m). Since the site is located right next to the sea, the groundwater level was high and varied from GL -3 m to GL - 4.1 m due to the tidal effect. The electrical resistivity image profile (RIP) of the reclaimed land at the test site is shown in Figure 2. The silty sand layer (backfilled sand layer) from GL -2 to -7 m has a much lower electrical resistivity. It indicates a higher water content and looser density of this layer.

2.1. Pounding Plan of the Pilot Test

The pilot test site covered an area of 20 x 20m^2. The layout of the pounding points is shown in Figure 3. The DC pounding work was divided into three stages to avoid excessive pore water pressure built up in the ground. As planned, the first and second stages were to be pounded 25 times per stage; the third stage was pounded 20 times. Pounding point was 10 m spaced at each stage. The pounding energy per impact was about equal to 500,000 kg-m with a 26,400-kg hammer and 19 m free fall (Chow, 1992). The hammer has a square shape footprint of 1.75 x 1.75 m in dimension and the height

of 2 m. After pounding, a crater was formed on the ground surface, and its volume was measured by traditional measuring method (i.e., only measure the depth and top diameter of the crater with rulers) and by the photogrammetry method.

Meanwhile, the rapid impact compaction (RIC) method was also tested here. RIC is a track-mounted machine that imparts energy by dropping an approximately 7,500 kg weight from a falling height of about 1 m onto a 1.5 m diameter steel plate that is placed on the ground surface. The time interval between each blow was 1.2-1.5 sec, and the impact rate was about 40-50 blows per min. In each pounding points, several sets of pounding were performed. One set of pounding means the hammer assembly has penetrated to the predetermined depth, or the hammer blow has reached the maximum number. In this test, the maximum blow number was set to 15 ~ 40 blows and the predetermined penetration depth is limited to 0.9 m. RIC has its onboard data acquisition system that automatically records information such as drop height, number of blows, and penetration per blow during the compaction process (Simpson, 2008).

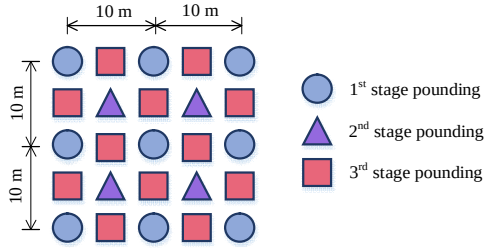

Figure 3. Layout of pounding points for different pounding stages

Table 2. Design requirement of SPT-N values after dynamic compaction

Depth (m)	SPT-N
GL ~ GL -5 m	>16
GL -5 m ~ GL -8 m	>19
GL -8 m ~ GL -10 m	>21

The traditional survey work carried out on this site includes the ground surface elevation survey around the crater and the volume of the crater. The ground surface survey was carried out by a level survey on the mark points set on the ground surface (Figure 5). The crater depth might be measured when the hammer is still inside the crater or lifted out of the crater. Its purpose is to calculate the heave and sag volumes around the crater. The area that calculated in the crater volume approach is the area of a grey area in Figure 5. The heave volume is calculated where the heave of the ground surface is significant.

$$V_h = \frac{\pi}{3} h_1 (D^2 + 3aD) \quad (1)$$

Where:
V_h = heave volume (m^3)
h_1 = highest height of measured heave (m)
D = distance of affected heave area (m)
a = radius of the crater (m)

So the pound-in volume resulted by the DC pounding (Figure 6a) can be obtained to evaluate the densification effect of DC to the ground soil.

$$V_p = V_c - V_h \quad (2)$$

Where:
V_p = pound-in volume
V_c = crater volume
V_h = heave volume

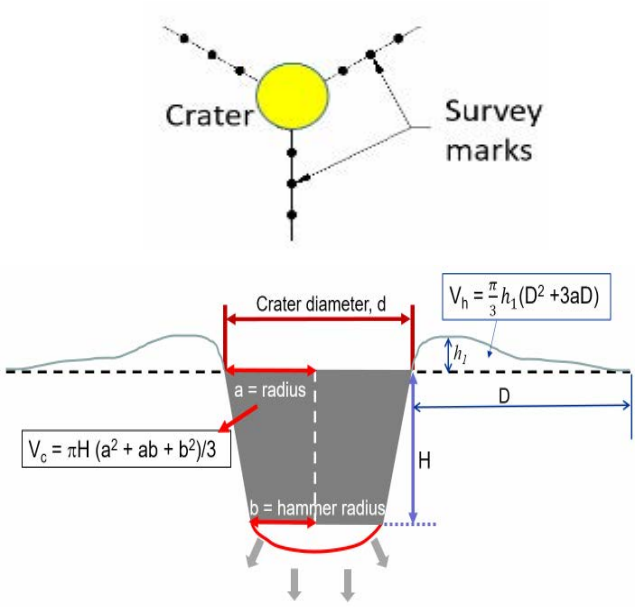

Figure 5. Field surveying work for ground heave and crater volume

The evaluation of densification effect is typically done by using the relationship among accumulated pound-in volume and heave volume (Note: plus backfill volume if backfill material is added during pounding) and some impacts. Tang (2016) measured the DC crater volume in each impact pounding. As shown in Figure 6c, the heave volume remained unchanged until it reached the 27th impact; after 27th impact, the ground heave began to increase, and the densification effect of DC began to decrease. This information can be provided to engineer to decide the optimum number of DC impact from the pilot test. However, there are two distinct problems here. Firstly, it needs to do the survey work after each DC impact. As shown in Figure 6b and Eq. 5, to obtain the pound-in volume and heave volume of the i^{th} impact pounding, an i^{th} run of survey needs to carry out, and the measurement results of $(i-1)^{th}$ impact pounding are needed. It is a very time-consuming surveying process for the pilot test. Secondly, it is not easy to measure the volume of crater and ground heave with reasonable accuracy using the traditional surveying method (Tang, 2016).

$$V_{p,i} = (V_{c,i} - V_{c,i-1}) - V_{h,i} \quad (3)$$

Where:
$V_{p,I}$ = pound-in volume at i^{th} number of pounding
$V_{c,I}$ = crater volume at i^{th} number of pounding
$V_{c,i-1}$ = crater volume at $(i-1)^{th}$ number of pounding
$V_{h,I}$ = heave volume at i^{th} number of pounding

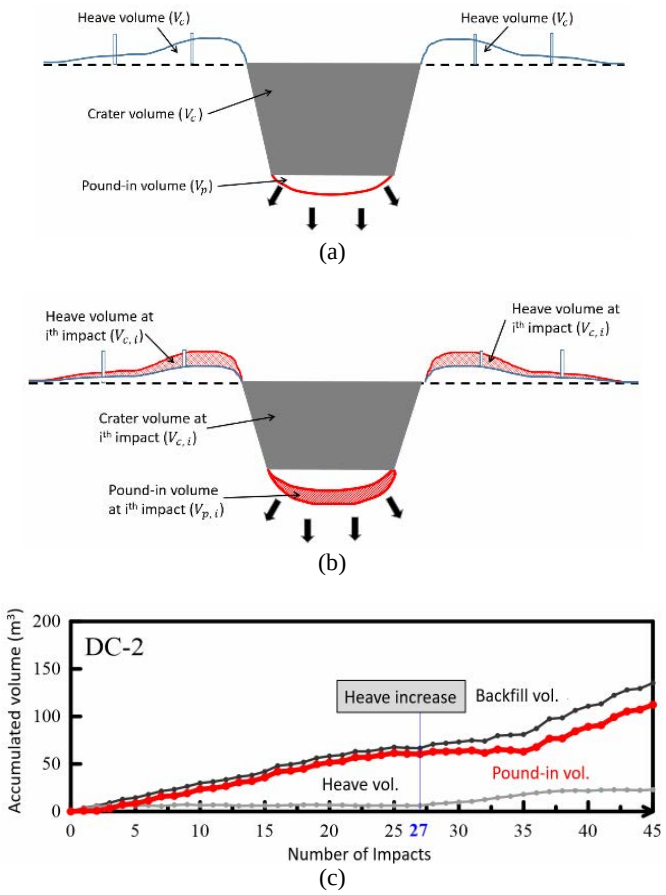

Figure 6. Measurement of heave volume and pound-in volume from the site surveying after DC pounding (Tang, 2016)

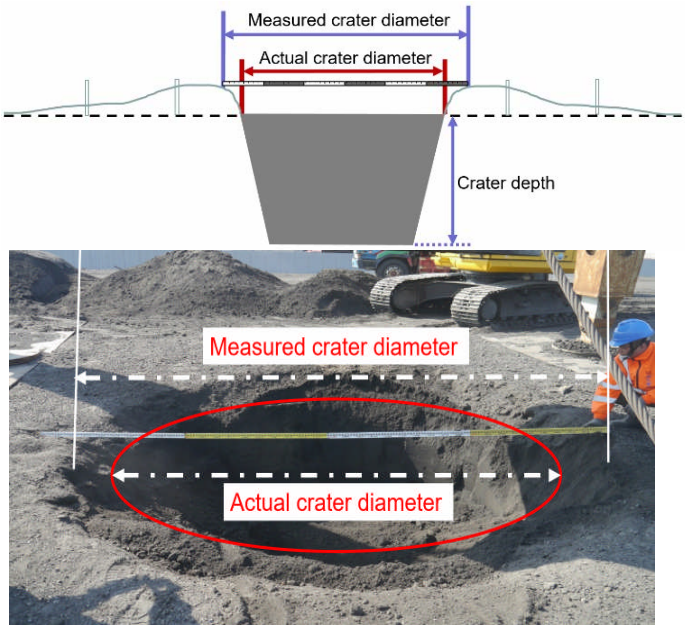

Figure 7. Problems associated with crater volume measurement in the traditional measuring method

As shown in Figure 7, the rim of crater appears on the ground is not the actual rim of the crater. Therefore, the measured crater diameter will be larger than the actual crater diameter. As a result, it will overestimate the crater volume and the densification effect of the DC. There is a need to have a more accurate and quicker surveying method for the crater. Preferably, this can be done with simple devices and at least effort.

2.2 Photogrammetry method

Recently, many image processing programs are available for UAV or drone to map specific area or landscape from the sky. These programs use the photogrammetry technology to process the captured images. The digital images of an area captured by drone were put into the software to get the 3D digital mapping of the area including the elevation and plane dimension of the building or landscape. The process of photogrammetry starts with capturing images from at least two different locations, then common points are identified on each image and rays line are developed from each camera angle to points on the object. These rays are intersected to produce 3D coordinates of the points of interest. (Li, 2016)

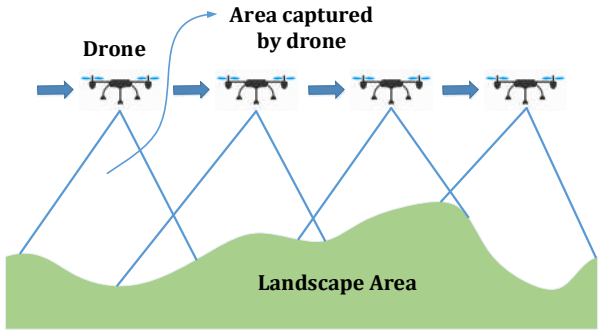

Figure 8. UAV or drone used to capture pictures for the photogrammetry

This study attempts to apply the photogrammetry method and use the commercial image processing software to the smaller object: the DC and RIC-induced craters. Digital images of the crater are taken on site by a smartphone or digital camera. Then these images put into the Pix4Dmapper software to generate a 3D point cloud model of the crater. The volume of the crater can be computed using the generated 3D model.

3. IMAGE PROCESSING

3.1 Point Cloud Model

The core of photogrammetry method is to generate a 3D object model by using the captured surface images of the object. The image processing software converts images into 3D models and point clouds. Having the point cloud data (e.g., the crater), the volume of the crater and the elevation change of the surrounding ground surface can be calculated.

3.2 Image Acquisition Plan

To establish the point cloud of the object, the number of digital images taken on the site should be from various angles to visualize its point clouds. Then the point clouds are used to reconstruct the model from the initial digital image. To obtain good images for processing, digital images should be taken around the object. It requires each image to overlap with its neighboring image to get high accuracy results. The higher the overlapping image rate, the more clear model can be constructed. The sufficient distance (ground sampling distance, GSD) of taking digital images should be carefully considered, and GSD serves as necessary measurement calculation. Therefore, it is crucial to make a good image acquisition plan to capture images at various angles and distances. (Pix4D, 2017)

The GSD is the distance between the center of two consecutive pixels on the ground. It influences the accuracy and the quality of the results as well as the details that are visible in the final results. GSD related to the camera height and camera properties. Therefore, the image acquisition plan should maintain at least two different camera height. While the image acquisition plan for the crater

depends on the GSD and overlap, the overlap of pictures depends on the affected area of the crater. In this case, crater volume and ground heave will be measured; overlapped images should contain all the area affected by the pounding. For crater volume and ground heave measurement, the following circular image acquisition plan is recommended:

(1) Moving around the crater for the first time with a camera dip-angle of 60°.
(2) Moving around the crater for the second and/or third time while reducing the camera height and the dip-angle in each round.
(3) It is best to take an image every 5 to 10 degrees when walking around the crater and take pictures to ensure enough overlap. More images should be taken for shorter distances. Recommended overlap is at least 75% of common points. The camera should be at a constant height above the crater as much as possible to maintain the GSD value.

3.3 Digital Image Processing

Since the images acquisition needs to change camera heights and angles, a length adjustable monopod was used to take pictures while walking around the crater. The images taken must cover the whole crater and also the possible heaving area around it. To enhance the stability of smartphone/digital camera and to assure better image overlapping, a DJI OSMO Mobile® was used here. OSMO Mobile® can also maintain the camera angle by its built-in gimbal and facilitate the process of image taking on site.

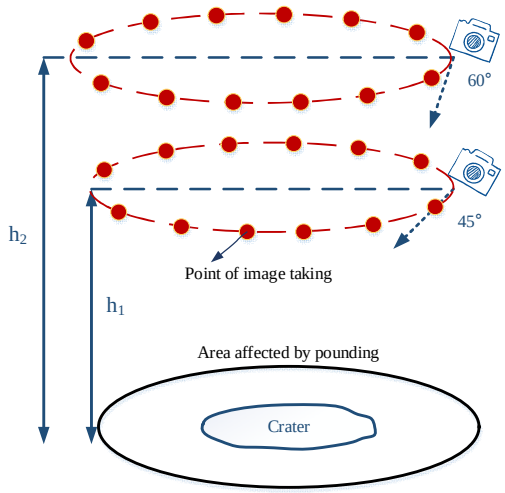

Figure 9. Image acquisition plan for crater measurement

After mounting the smartphone/digital camera to the OSMO Mobile, the joystick handle was used to control the camera function of the smartphone. For the maximum use, the extension rod of OSMO Mobile was also used to get the additional height of the images. The process of crater images acquisition includes (1) adjust and fix the smartphone/camera angle, (2) hold the camera to the first height (h_1), (3) walk step by step around the crater and take digital pictures at each walking step. Carry out another round with different camera angle and height.

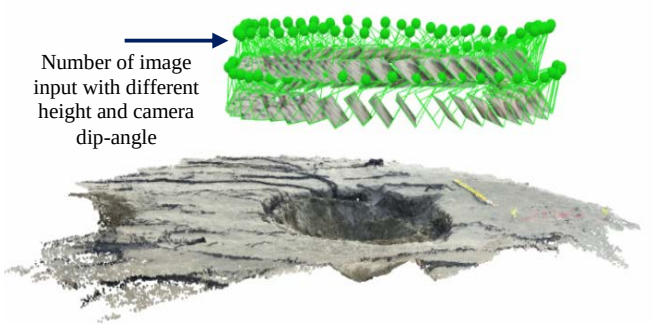

Figure 10. Generated point cloud model by the image acquisition plan

Following are the standard operation procedures (SOP) of digital image processing adopted in this study:

(1) Input digital images
Based on the image acquisition plan, digital images are obtained from the site. Input digital images to the Pix4Dmapper software. Select Processing option of 3D Maps, and start processing.
(2) Processing Step 1: Initial Processing
Select the Initial Processing option, and click start. When start Step 1, Pix4Dmapper computes the key points on the images. It uses these key points to find matches between images.
(3) Processing Step 2: Point Cloud and Mesh
After Step 1 Initial Processing is completed, Step 2 Point Cloud and Mesh can be processed. Select Point Cloud and Mesh option. Click start to begin Step 2 processing. In this step, the point cloud is generated and can be visualized in rayCloud.
(4) Scale the Model
After finish Step 2, the initial point cloud data are generated. However, these data need to be adjusted using the scale or ground control points (GCPs) on site. Once the point cloud has been adjusted with the scale, it needs to be reoptimized. After re-optimization, the processing of Step 2 is re-generated.
(5) Processing Step 3, DSM, Orthomosaic and Index
DSM (Digital Surface Model) is a 2.5D model of the mapped area. Each pixel and each point of the vector point cloud contain (X, Y, Z) information. Running Step 3 means that there is information about the coordinate of the measuring object. After processing Step 3, the volume of the crater can be obtained. Select the area of interest and click Compute.

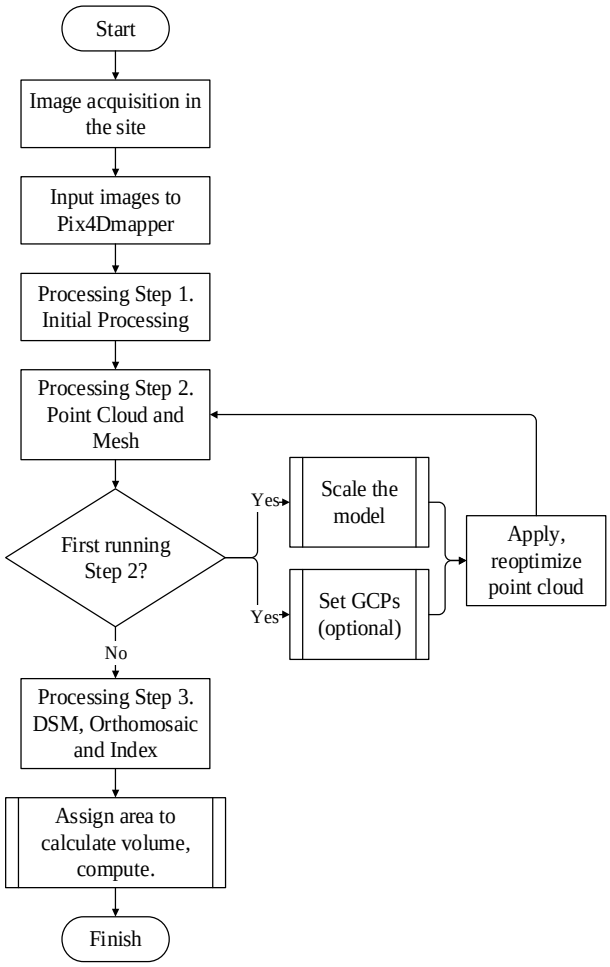

Figure 11. Standard operation procedure (SOP) of digital image processing using photogrammetry software

4. VOLUME MEASUREMENT

4.1 Calibration Box

To calibrate the accuracy of volume measurement, a box with known dimension is used here as the sample object to check the accuracy of volume measured by this photogrammetry method. The dimension of the box is 28.5 x 16.5 x 6.8 cm (Figure 12) with the inside volume of 2894.74 cm^3. Unfortunately, the default unit "meter" used in Pix4Dmapper cannot be changed on the computer screen, and the output value of measured volume can only be displayed to two decimal places. As a result, the output volume of the calibration box from Pix4Dmapper is 0.00 m^3. It is unacceptable for the volume measurement here. To deal with this problem, the default unit of the software is disregarded, and the metric unit in the software is regarded as "cm". Fortunately, this change on the default unit did not affect the operability of volume calculation of this software. Figure 13 shows the volume determined for the box using the Pix4Dmapper software.

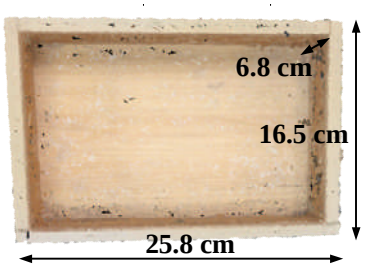

Figure 12. Point cloud image of the calibration box

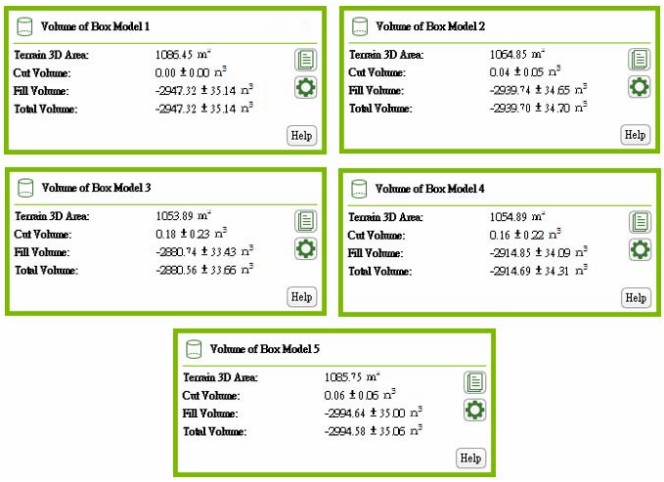

Figure 13. Volume measurement result of the calibration box using Pix4Dmapper software

The volume of the box was measured five times by the photogrammetry method following the standard operation procedures (SOP) mentioned above. On Step 3, different measured volumes of the box were found among the five measurements (Table 3). Such a difference in measured volume were mainly resulted from the process of manual selection of box boundary from the point cloud data. Slightly different box boundary may be selected from different runs of measurement. The average volume obtained from the output is 2935.37 cm^3; while the actual inside volume of the box is 2894.74 cm^3. The standard deviation of the five-volume measurements was 42.13 cm^3. Compared to the actual volume of the box, the error is only 1.5% of the box volume (Table 3). Such an error should be acceptable for the heavy pounding induced crater volume measurement. It confirms that this photogrammetry method and Pix4Dmapper software are applicable to the volume measurement of a smaller object (like the calibration box and the crater) using a smartphone/digital camera.

Table 3. The standard deviation of the box volume measurement

Volume No.	Volume (cm^3)	Mean (cm^3)	Deviation (cm^3)	Standard Deviation (cm^3)	% of Error* (%)
1	2947.32	2935.37	11.95	42.13	1.46
2	2939.70		4.33		
3	2880.56		-54.81		
4	2914.69		-20.68		
5	2994.58		59.21		

$$*\%\ of\ error\ = \frac{42.23}{2894.74} \times 100 = 1.46\% \approx 1.5\%$$

4.2 Photogrammetry Measurement of Craters

In the pilot test site, both DC and RIC craters were measured with the photogrammetry method following the above mentioned image acquisition plan. Not only the crater volume but also the ground heave were measured. The captured images covered an area which was large enough to cover the ground control points (GCPs) around the crater and also the surrounding ground heave. In addition, both the digital images before and after DC pounding were taken and compared. GCPs adopted here were with known coordinates and to be used for creating the initial coordinates and measure the elevation change of ground surface caused by DC pounding.

Following are the steps of this photogrammetry procedure adopted for the crater measurement:

(1) **Taking images of initial site condition**. In each impact location, at least three points are marked on the ground surface and used as GCPs. One of the GCPs is used as the benchmark and assigned the initial coordinate of (0,0,0). The coordinates of the other GCPs should be decided based on their distances and directions to the benchmark GCP. It is essential to make sure that these GCPs cannot be moved during DC pounding. They are supposed to work as permanent GCPs (Figure 14).

Figure 14. Images acquisition process of the initial site condition with its GCPs (Ground Control Points)

(2) **Taking images after-pounding**. The images captured after pounding should cover not only the crater but also the GCPs. Therefore, the elevation difference before and after pounding can be compared and calculated (Figure 15).

Figure 15. Images acquisition process after-pounding

(3) **Processing images of the initial site condition**. Input the images data of initial site condition to the software and run the process. Get the point cloud data of the initial site condition. Input the coordinate of benchmark GCP (0,0,0) and also the other GCPs. Each GCP needs to be precisely clicked on at least three images of the point cloud. Input the adjusted GCPs then re-optimize the point cloud (Figure 16).

Figure 16. Setting the GCP point coordinate and selecting in the at least three images

(4) **Set elevation of the initial site condition**. After the point cloud has been re-optimized, the elevation of the ground surface can be set. Choose the area of interest which will cover the crater and its surrounding area and export as shapefiles (.shp). The elevation of the selected area will be set as the initial elevation for the calculation of crater volume and ground heave afterward.

(5) **Processing after-pounding condition**. Input the images captured after the first pounding. Since the GCPs do not move, the GCP coordinates for after-pounding are the same as the initial site condition. Repeat the process adopted for the initial site condition to get the point cloud of the first pounding.

(6) **Crater volume measurement**. Import the shapefiles (.shp) of the initial elevation and then compute the crater volume. At the same time, the ground heave can also be calculated (Figure 17).

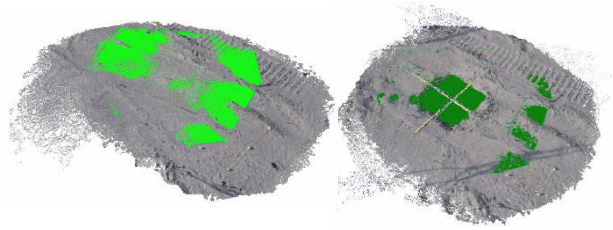

(a) (b)

Figure 17. (a) Selected elevation area on initial condition that exported as shapefiles (b) Volume measurement with imported shapefiles after pounding

4.2.1 Point Cloud of Craters

Figures 18 and 19 show the pictures of the first stage RIC crater after two sets of pounding. The RIC craters mostly have a shape close to a conical shape which is different from the real shape of the crater formed by RIC pounding. Because, after each set of RIC pounding, the hammer assembly of RIC was lifted up from the crater. In the process, it also brought out some soil with it and formed a crater with an upside down conical shape.

Figure 20 and 21 show the pictures of third stage DC craters and their point cloud models (Crater D3). It can be seen from the picture that the shape of the crater is irregular, but is close to conical or truncated conical shape. The conical shape assumption can be confirmed by the cross-section of the point cloud model shown in the figures. The white cross shown in the picture is the ruler used to measure the top diameter of the crate during traditional crater measurement. The intersection of the cross was used to locate the measuring location for the crater depth. The yellow ball inside the crater was used to keep the camera focus on the crater during images capturing process.

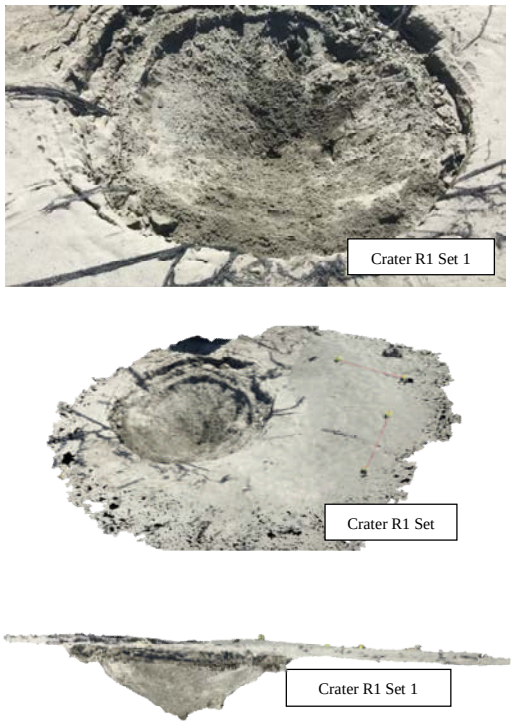

Figure 18. (a) Photo taken at the site, (b) Point cloud model (bird's eye view), (c) Point cloud model (cross view) of the third stage of RIC crater (R1) at first set

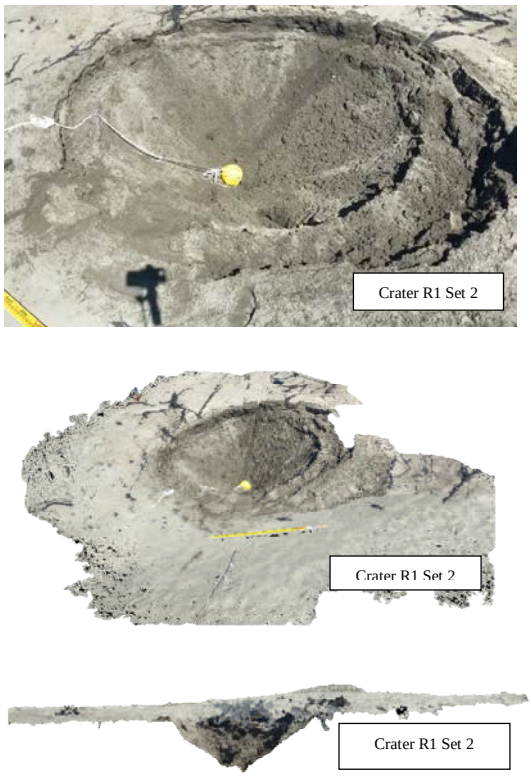

Figure 19. (a) Photo taken at the site, (b) Point cloud model (bird's eye view), (c) Point cloud model (cross view) of the third stage of RIC crater (R1) at the second set

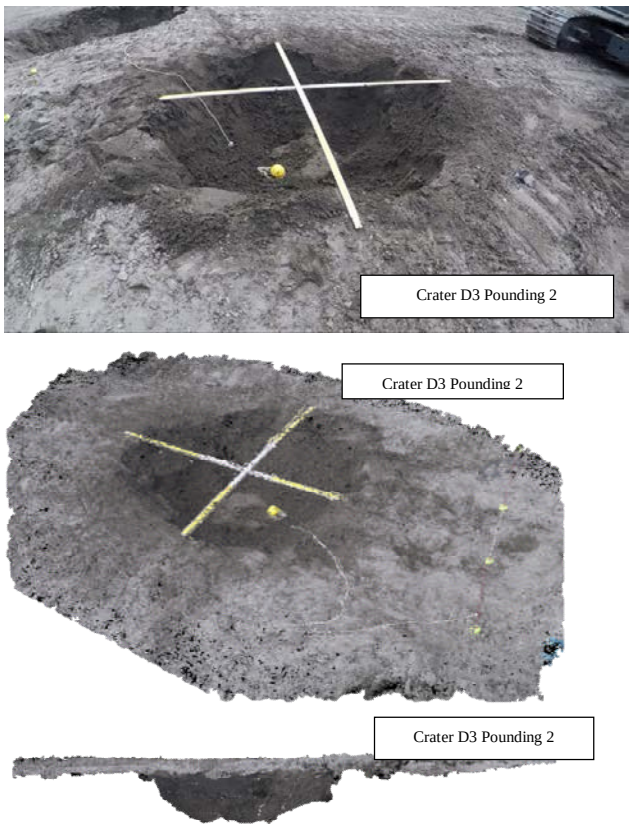

Figure 20. (a) Photo taken at the site, (b) Point cloud model (bird's eye view), (c) Point cloud model (cross view) of the third stage of DC crater (D3) at second pounding

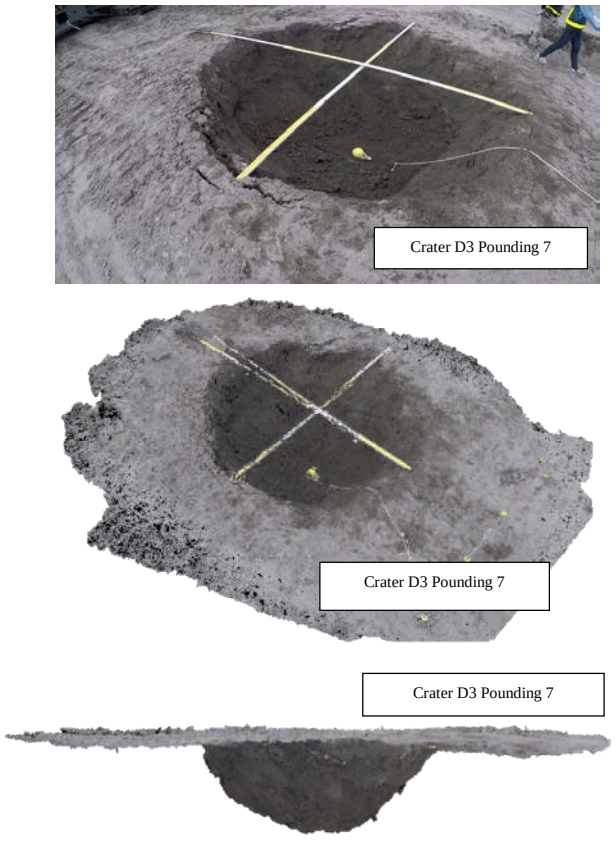

Figure 21. (a) Photo taken at the site, (b) Point cloud model (bird's eye view), (c) Point cloud model (cross view) of the third stage of DC crater (D3) at seventh pounding

4.2.2 Craters Volume Measurement

On the site, crater volume was measured with the traditional surveying method as well as the photogrammetry method. For the former, measuring rulers (Figure 7) was used to measure the depth and top diameter of the crater; for the latter, smartphone or digital camera was used to capture the images of the crater and the GCPs around it (Figure 15). The craters were measured after the DC hammer was lifted out. Without the hammer in the crater, the soil on the side of the crater would fall off and changed the apparent shape of the crater from truncated conical to more or less conical. Nevertheless, it was only the shape changed, and the volume of the crater may not change much.

The dimension of RIC craters measured from the traditional surveying method yielded the top diameters ranging from 1.5 to 3 m and depth from 0.5 to 0.9 m. The top diameter of DC craters ranged from 2.5 to 5.0 m and depth from 0.5 to 2.0 m. Since the RIC crater is notably smaller than DC, it requires less amount of images than those of DC crater.

For the photogrammetry method, several trial and error tests had been performed. The first trial was to determine the adequate input number of images while considering the processing time and accuracy of crater volume measurement. The initial trial number of input images starts from 40. However, 40 picture images were not enough to generate a point cloud model and some of its details outside the crater, where the GCPs were usually located, were missing. Thus the ground heave outside the crater cannot be shown. Until the number of input images reached the threshold value of 110 for DC and 70 for RIC, the point cloud model started to show the complete crater details and ground heave around it. However, the threshold input number of the images tends to differ from one crater to another. Since each crater has its details and needs different threshold images to generate the point cloud model, the processing time to generate the point cloud data varies. In addition, the processing time also depends on the CPU of the computer and the number of input images. Based on the experienced obtained from this study, the processing time is around 20-27 minutes for RIC craters and 30-45 minutes for DC craters (Note: 110 images needed for DC and 70 images for RIC).

After the threshold number of images had been decided and the point cloud and 3D models of the site could be generated and scaled, then the crater volume could be computed. Since most of the craters did not show significant ground heave, so the volume change mainly results from the forming of the crater. The traditional measuring method only measures the depth and top diameter of the crater. It is not easy to accurately measure the volume of the crater with such limited data especially the shape of craters is irregular. To simplify the volume calculation of the crater, the traditional measuring method uses the following formulas to approximate the crater volume. Among them, Eq. 4 formula is for the cone shape crater; Eq. 5 is for the truncated cone shape crater. As shown in Figure 5, Eq. 5 is the commonly used formula to calculate the volume of the truncated cone shape DC crater.

$$V_{c1} = \frac{\pi r^2 h}{3} \tag{4}$$

$$V_{c2} = \frac{\pi h}{3}(a^2 + ab + b^2) \tag{5}$$

Where:

V_{c1} = volume of the crater with a conical shape
V_{c2} = volume of the crater with a truncated conical shape
r = radius of crater measured on site
a = on-site measured top radius of the crater
b = effective radius of hammer footprint = 1.0 m (converted from square to circular shape by means of equivalent area method)
h = measured depth of the crater

The volume calculated from the photogrammetry method ($V_{c,p}$) and field measurement (V_{c1} and V_{c2}) are listed in Tables 4 and 5. In total, 3 RIC craters (R1, R2, and R3) and 3 DC craters (D1, D2, and D3) are listed here. R1 and D1 represent the 1st stage pounding (refer to Figure 3) for RIC and DC; R2 and D2 are for the 2nd stage pounding; R3 and D3 are for the 3rd stage pounding. In general, the ground becomes stronger when the compaction proceeds from the first stage to the third stage. So the crater volume reduces as the impact stages escalate.

For the RIC cases, each crater was subjected to two impact sets; each set has 15-40 blows. As mentioned before, the RIC resulted craters can only be measured after completion of each set, and the craters are generally in a conical shape. Therefore, only V_{c1} formula is used to calculate the volume of RIC craters based on the field measured crater depth and top diameter from the traditional measuring method. The point cloud data generated from Pix4Dmapper software for the RIC craters are shown in Figure 22. The comparison between crater volume determined from photogrammetry method (Pix4Dmapper) and traditional measuring method is shown in Figure 23.

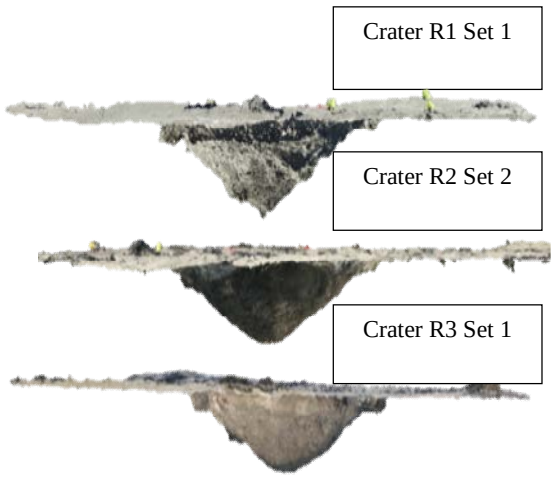

Figure 22. 3D model from point cloud data representative of each stage RIC craters (cross views)

Table 4. Comparison of RIC crater volume between Photogrammetry and traditional field measurement

Crater No.		Photogrammetry Measurement		Traditional Field Measurement			
		Crater Volume ($V_{c,p}$)	Heave Volume ($V_{h,p}$)	Depth (h)	Top dia. (2r)	V_{c1}	$\frac{V_{c1}-V_{c,p}}{V_{c,p}}$
		m^3	m^3	m	m	m^3	%*
R1	1	1.60	0.08	0.88	3.00	2.073	29.6%
	2	1.25	0.02	0.70	2.40	1.056	-15.6%
R2	1	1.57	0.01	0.84	2.55	1.430	-8.9%
	2	1.67	0.05	0.80	2.93	1.798	7.7%
R3	1	1.40	0.02	0.83	2.38	1.231	-12.1%
	2	0.95	0.16	0.53	1.85	0.475	-50.0%

* "-" means crater volume is underestimated

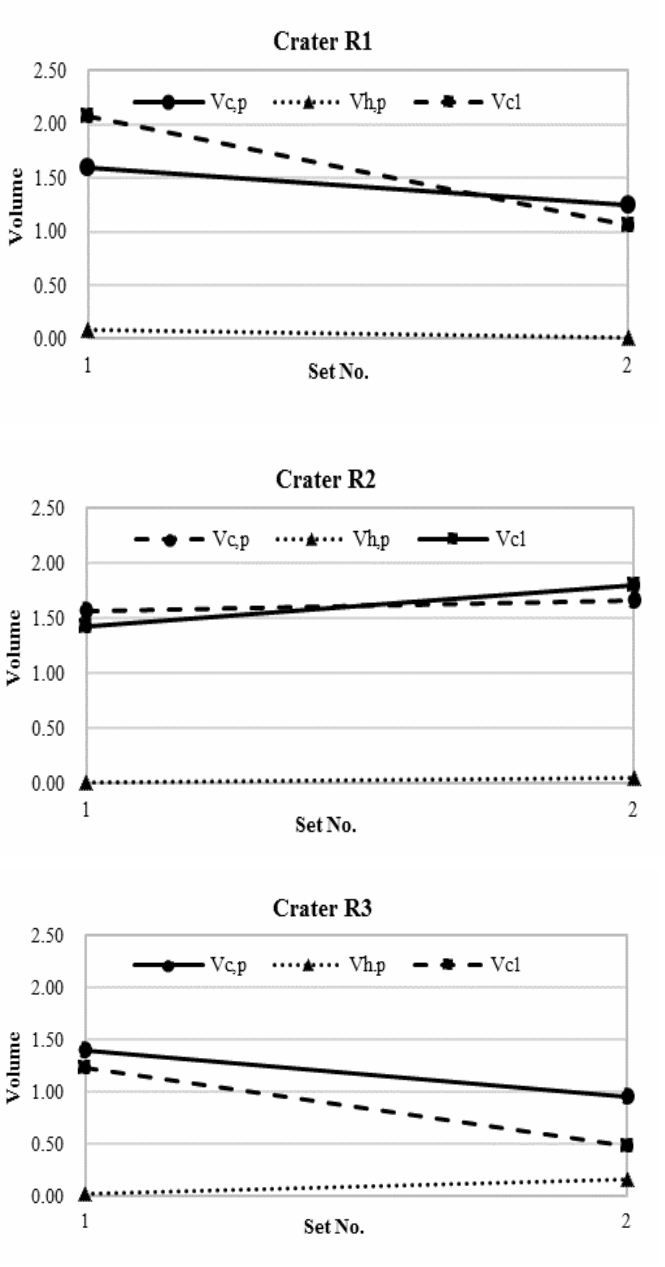

Figure 23. Comparison graphs between photogrammetry and field measurement of RIC craters

For the DC cases, each pounding stage had 20-25 poundings, but only the first ten poundings are shown in Table 5. The DC hammer used in this case had a square shape footprint (Figure 24). However, during the free fall process, the hammer tends to rotate a little during each pounding and forms a more or less circular crater on the ground surface after a few impacts (Figure 24). The crater resulted by this DC hammer can be somewhat in a cone shape or truncated cone shape except for the 1st impact. As the number of impact increases, the crater depth increases. However, the crater shape remains close to conical. Together with the on-site measured depth and a top diameter of the crater, Eq. 4 and 3 were used to calculate the crater volume. Craters (D1, D2, & D3) from different pounding stages were chosen for comparison here.

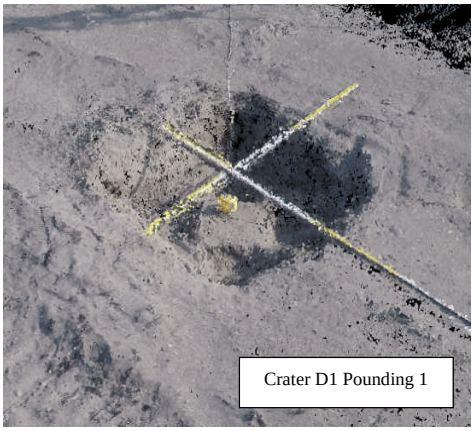

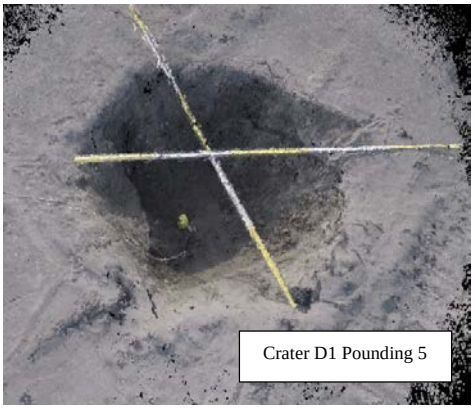

Figure 24. 3D model from point cloud data of a DC crater for different pounding (birds-eye view) (contd.)

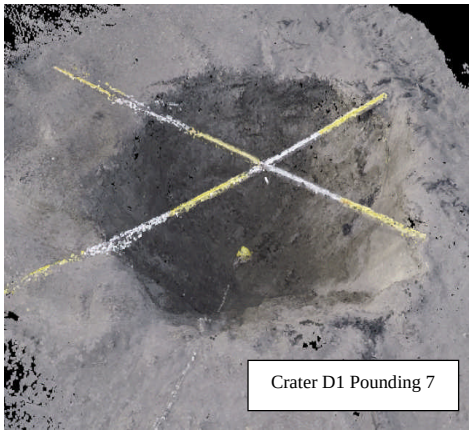

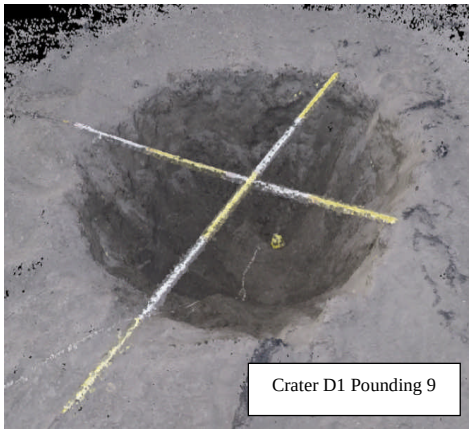

Figure 24. 3D model from point cloud data of a DC crater for different pounding (birds-eye view)

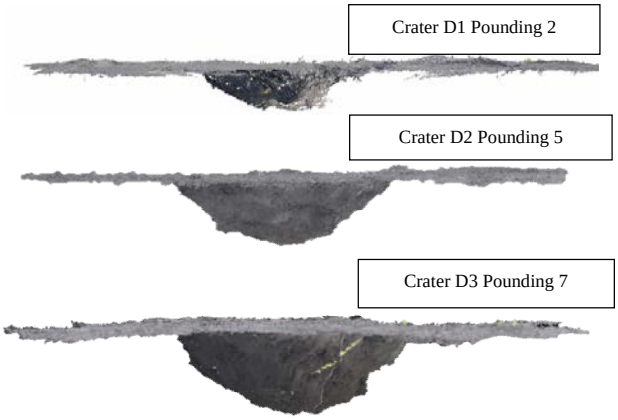

Figure 25. 3D model from point cloud data representative of each stage DC craters (cross view)

The methods (traditional measuring and photogrammetry) used for the DC crater measurement are the same as those for the RIC craters. However, the craters formed by DC tend to be much larger due to larger pounding energy. Therefore, the area size to be covered by the photogrammetry method is larger and more images are needed to generate the point cloud model after each DC crater measurement. The results of DC craters measurement are discussed in the following section.

Table 5. Comparison of DC crater volume between photogrammetry and traditional field measurement

Crater No.		Photogrammetry Measurement		Traditional Field Measurement					
		Crater Vol. ($V_{c,p}$)	Heave Vol. ($V_{h,p}$)	Depth (h)	Top Dia. (2r)	V_{c1}	$\frac{V_{c1}-V_{c,p}}{V_{c,p}}$	V_{c2}	$\frac{V_2-V_{c,p}}{V_{c,p}}$
		m^3	m^3	m	m	m^3	%*	m^3	%*
D1	1	1.42	0.24	0.44	2.10	0.508	-64.2%	1.598	2.3%
	2	1.79	0.49	0.67	3.05	1.632	-8.8%	3.658	90%
	3	2.19	1.00	0.92	3.35	2.703	23.4%	5.644	141%
	4	2.74	0.51	1.05	3.30	2.994	9.3%	6.320	116%
	5	4.04	0.24	1.13	3.40	3.420	-15.4%	7.064	63.7%
	6	4.66	0.31	1.28	3.50	4.105	-11.9%	8.307	67.2%
	7	4.95	0.42	1.31	3.65	4.569	-7.7%	8.983	70.6%
	8	5.63	0.38	1.39	3.65	4.848	-13.9%	9.531	59.2%
	9	6.11	0.46	1.44	3.80	5.444	-10.9%	10.42	60.7%
	10	7.38	0.13	1.57	3.75	5.780	-21.7%	11.16	42.4%
D2	1	1.34	0.44	0.40	2.10	0.511	-61.8%	1.527	4.0%
	2	2.76	0.24	0.72	3.05	1.150	-58.3%	3.087	2.7%
	3	3.67	0.14	0.95	3.35	2.390	-34.9%	5.290	34.2%
	4	4.51	0.10	1.16	3.30	3.287	-27.1%	6.955	44.1%
	5	4.62	0.38	1.25	3.40	3.783	-18.1%	7.815	58.4%
	6	4.82	0.73	1.34	3.50	3.937	-18.3%	8.220	59.6%
	7	4.80	1.60	1.50	3.65	4.674	-2.6%	9.555	86.6%
	8	5.97	1.30	1.51	3.65	5.296	-11.3%	10.39	63.7%
	9	6.84	0.21	1.61	3.80	6.411	-6.3%	12.06	66.4%
	10	7.02	0.29	1.63	3.75	5.842	-16.8%	11.38	52.5%
D3	1	1.47	0.21	0.68	2.24	0.893	-39.2%	2.632	63.5%
	2	2.05	0.10	1.06	2.75	2.099	2.4%	5.121	131%
	3	2.24	0.08	1.22	3.20	3.271	46.0%	7.065	194%
	4	2.77	0.11	1.21	3.34	3.534	27.6%	7.395	150%
	5	3.65	0.39	1.25	3.33	3.629	-0.6%	7.610	95%
	6	3.85	0.19	1.42	3.35	4.172	8.4%	8.711	112%
	7	4.22	0.08	1.41	3.55	4.652	10.2%	9.322	107%
	8	4.74	0.09	1.48	3.70	5.304	11.9%	10.33	105%
	9	4.62	0.04	1.60	3.72	5.797	25.5%	11.25	129%
	10	5.15	0.15	1.56	3.77	5.805	12.7%	11.16	104%

* "-" means crater volume is underestimated

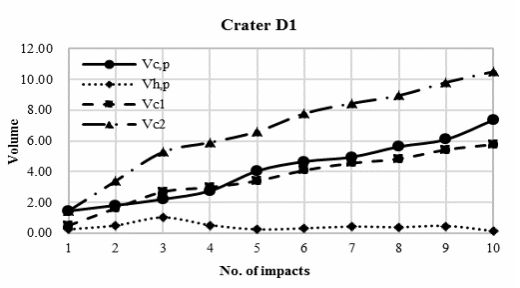

Figure 26. Comparison between photogrammetry and field measurement of DC crater volume (contd.)

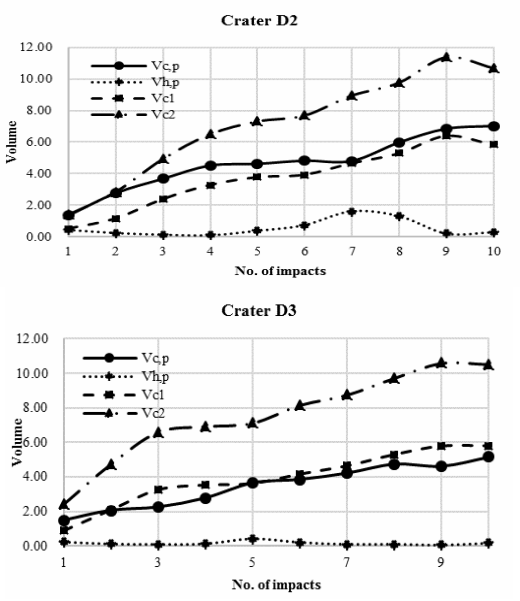

Figure 26. Comparison between photogrammetry and field measurement of DC crater volume

5. DISCUSSION ON MEASUREMENT RESULTS

It can be found from the RIC craters that for the first and second stages poundings, the crater volume determined from the traditional measuring method yields a larger volume for Set 1 and a smaller volume for Set 2 compared to those measured from Pix4Dmapper. Apart from the overestimation of top diameter by traditional measuring method, one other possible reason for this phenomenon is that the traditional measuring method used the ruler to measure the crater depth (h). The contractor tended to push the ruler with force into the bottom of the crater. So the measured crater depth (h) was larger than that measured by photogrammetry method which only measured the surficial shape of the crater. Thus, the volume calculated with either Eq. 4 or Eq. 5 showed a larger volume using the traditional method. After one set of RIC pounding, the crater was backfilled with soil before performing next set of pounding. Since the ground became denser as the pounding increased, it became more difficult to push the ruler into the bottom of the crater. As a result, the measured depth of crater was closer to the photogeommetry method, so was the crater volume approximated by Eq. 4 and 5. Therefore, the crater volume measured with traditional method reduced and became less than that obtained from the photogrammetry method (Figure 23). At the third stage, the above mentioned effect of over-estimating crater depth disappeared. The volume (V_{c1}) of R3 crater became less than $V_{c,p}$ for both set 1 and set 2. However, the assumption made on the shape of the crater may be the other source of volume underestimation. In other word, assuming a conical shape for the crater and using the traditional measuring method can under-estimate the crater volume by 12~50% (Crater R3 in Figure 23).

As for DC case, the crater volumes calculated from Eq. 4 and 5 are compared with those calculated by photogrammetry method. As shown in Table 5 and Figure 26, the crater volume calculated from Pix4Dmapper software is in better agreement with Eq. 4 for conical shape crater with the maximum difference of 65%. The larger difference appears in the initial impacts. As the number of impacts increased, the crater shape became closer to conical; then the difference can be reduced to about 20%. In comparison, the crater volume calculated from Eq. 5 (Note: the most commonly used formula used by the DC contractors) tends to overestimate the volume of DC crater by more than 65%. It implies that if the hammer was not in the crater during crater measurement, the truncated conical shape assumed for the crater by Eq. 5 could be quite different from the apparent crater shape and overestimates the volume of crater. So if the crater volume is used to evaluate the effectiveness of compaction as shown in Figure 6, such an overestimation on crater volume should be taken into account.

Also shown in Figures 23 and 26, the RIC and DC induced ground heave is not apparent in this pilot test. In other words, most of the compaction energy had been absorbed by the ground. It indicates that the in-situ ground and groundwater conditions underlying the site are suitable for either DC or RIC method.

6. CONCLUSIONS

Among the parameters monitored for DC or RIC method, the volume of the crater is the most significant one to evaluate the effectiveness of pounding. This paper presents a photogrammetry method which can carry out the volume measurement of the crater and the surrounding ground heave with better accuracy. The following conclusions are made based on the results of a field trial test on a hydraulically filled reclaimed site.

1. Before the field test, an accuracy of 98.5% on volume measurement of a calibration box with known volume had been obtained using the photogrammetry method and Pix4Dmapper software in the laboratory.
2. By using the smartphone or digital camera and the photogrammetry technology, the point cloud data of the ground surface can be established. Then, the point cloud data were further calibrated with the ground control points placed around the crater. The change of crater volume before and after each pounding can be determined using the calibrated point cloud data with reasonable accuracy.
3. By assuming a conical shape for the RIC crater, the crater volume calculated from Eq. 4 for the traditional measuring method tends to underestimate the crater volume by about 20% compared to that measured with the photogrammetry method. However, the conical shape may not be very representative to the real shape of the crater formed by RIC pounding due to the disturbance caused by lifting up the hammer from the crater.
4. DC crater volume measured by the photogrammetry method is in good agreement with that calculated from Eq. 4 (for conical shape crater). Although the overestimation by Eq. 4 is large in the initial impacts, the difference is reduced to about 20% as the number of impacts increased and the crater shape became closer to conical. In comparison, if Eq. 5 (truncated cone) is used to calculate the crater volume, more than 65% overestimation than that measured with photogrammetry method may result. However, it should be noted that the craters in this study were measured after the hammer was lifted up from the crater and the side of crater might fall off to the bottom and changed the apparent shape of the crater from truncated conical to more or less conical (Figure 25). If the crater were measured with the hammer still in the crater, the shape of the crater might more likely be in truncated conical shape. Then the overestimation in volume by Eq. 5 may not be as much as those shown in Table 5 and Figure 26.

7. ACKNOWLEDGMENTS

The Authors wish to thank the I-San construction company for carrying out the DC and RIC operation for the trial test of this crater volume measurement program. The financial support from the Ministry of Science and Technology (MOST) of Taiwan Government and Li-Jia Engineering Company are also greatly appreciated.

8. REFERENCES

Chow, Y. K., Yong, D. M., Yong, K. Y. and Lee, S. L. (1992). "Dynamic Compaction Analysis", *Journal of Geotechnical Engineering*, ASCE, 118(8), pp. 1141.

Li, L., Zhang, X., Chen, G. and Lytton, R. (2016). "Measuring Unsaturated Soil Deformations during Triaxial Testing Using a Photogrammetry-Based Method", *Canadian Geotechnical Journal*, NRC Research Press, 53, pp. 476.

Pix4D SA. (2017). Pix4Dmapper 4.1 User Manual, Switzerland, pp. 11-46.

Simpson, L. A., Jang, S. T., Ronan, C. E. and Splitter, L. M. (2008). "Liquefaction Potential Mitigation using Rapid Impact Compaction", *Geotechnical Earthquake Engineering and Soil Dynamics IV*, ASCE, pp. 5.

Tang, I. E. (2016). "Effect of Dynamic Replacement on the Engineering Properties of Coal Ash Pond", *Master's Thesis*, NTUST, Taipei, Taiwan